


Cite this: *RSC Adv.*, 2020, 10, 18407

Cytotoxicity and degradation product identification of thermally treated ceftiofur†

Hong Zhang,[‡] Shiyong Lu,[‡] Honglin Ren, Ke Zhao, Yansong Li, Yuting Guan, Hanxiao Li, Pan Hu* and Zengshan Liu*

Ceftiofur (CEF) is a cephalosporin antibiotic and is a commonly used drug in animal food production. As a heat-labile compound, the residual CEF toxicity after thermal treatment has rarely been reported. This study was to investigate the potential toxicity of thermally treated CEF and determine the toxic components. By cytotoxicity tests and liquid chromatography-mass spectrometry (LC-MS) assays, the cytotoxicity of the thermally treated CEF (TTC) and the components of TTC was identified, respectively. Our results showed that TTC exhibited significantly increased toxicity compared with CEF towards LO2 cells by inducing apoptosis. Through LC-MS assays, we identified that the toxic compound of TTC was CEF-aldehyde (CEF-1). The IC_{50} value of CEF-1 on LO2 cells treated for 24 h was $573.1 \mu\text{g mL}^{-1}$, approximately 5.3 times lower than CEF ($3052.0 \mu\text{g mL}^{-1}$) and 3.4 times lower than TTC ($1967.0 \mu\text{g mL}^{-1}$). Moreover, we found that CEF-1 was also present in thermally treated desfuroylceftiofur (DFC), the primary metabolite of CEF, indicating that residual CEF or DFC could produce CEF-1 during the heating process. These findings suggest that CEF-1 is a newly identified toxic compound, and CEF-1 may pose a potential threat to food safety or public health.

Received 8th December 2019

Accepted 6th May 2020

DOI: 10.1039/c9ra10289b

rsc.li/rsc-advances

1. Introduction

Antibiotics are widely used in livestock production to prevent disease and promote growth.¹ According to reports, approximately 70% of antibiotics are used in food producing animals² around the world. It is estimated that the consumption of antibiotics in livestock production will continue to increase as a consequence of growing demand for animal protein.³ Studies have showed that antibiotic residues in food can have adverse effects on humans.^{4,5} Thus, contamination of animal products with antibiotics has become an important threat to public health.

CEF is a third-generation animal-specific cephalosporin antibiotic which has broad activity spectrum due to its bulky imino-methoxy side chain.⁶ CEF has no mutagenicity biologically^{7–9} and possess a short drug withdrawal time. The preslaughter withdrawal time of CEF was four days in cattle or swine and zero days in milk cow, sheep or goats.^{10,11} Based on the high efficacy, safety and short drug withdrawal period, CEF has become one of the most commonly used antibiotics in animal husbandry to control infection and increase animal

production,^{12–23} especially for the treatment of mastitis in dairy cattle by intramammary (IMM).^{24–26} However, IMM CEF treatment of mastitis in dairy cows may result in the concentration of CEF in milk higher than the tolerance set by the FDA.^{27–30} CEF was reported to be the predominant violative residues which account for 29% in the United States.³¹ Thus, food safety issues caused by CEF residues should be fully studied.

Cooking procedure is important for the reduction of antibiotic residues in food.^{32,33} The majority of animal-derived foods, such as meat, can only be eaten by high-temperature cooking. In China or some countries, foods sometimes will be cooked for a long time to get delicious taste as well. However, like other β -lactams, CEF is an unstable antibiotic.^{34,35} Reports showed that CEF was highly unstable under high temperature condition (such as cooking process) and the degradation of CEF was time-dependant.^{36,37} Furthermore, CEF is susceptible to acidic, alkaline, and enzyme-catalyzed hydrolysis.^{6,38,39} Thus, the degradation and the potential toxicity of the thermally treated CEF (TTC) are topics worthy of study. In this paper, we investigated the cytotoxicity of the TTC, and further analyzed the components of the thermal degradation products of CEF and desfuroylceftiofur (DFC), which is the primary metabolites of CEF.²³

2. Materials and methods

2.1 Chemicals and reagents

Ceftiofur sodium (CEF, purity > 98%, CAS# 104010-37-9) was purchased from Meilunbio (China). Desfuroylceftiofur (DFC)

Key Laboratory of Zoonosis Research, Ministry of Education, Institute of Zoonosis, College of Veterinary Medicine, Jilin University, 5333 Xi'an Road, Changchun, Jilin, 130062, PR China. E-mail: hupan84@163.com; zslu1959@sohu.com; Tel: +86-431-8783-6716; +86-431-8783-6703

† Electronic supplementary information (ESI) available. See DOI: 10.1039/c9ra10289b

‡ These authors contributed equally to this work.



was obtained from Toronto Research Chemicals (Canada). RPMI 1640, DMEM and MEM culture medium were provided by Gibco (USA). Fetal bovine serum (FBS) was purchased from BI (Israel). Cell Counting Kit-8 (CCK-8) was obtained from Dojindo (Japan). Hoechst 33342/PI fluorescent dye, JC-1 probe and trypsin were provided by Solarbio (China). Annexin V-FITC/PI apoptosis kit was purchased from BD (USA). High-performance liquid chromatography grade acetonitrile and formic acid were obtained from Tedia (USA).

2.2 Preparation of test substances

CEF was diluted in distilled water resulting in a stock solution at concentration of 100 mg mL^{-1} and kept in the dark at -20°C . Stock solution was thawed at room temperature and diluted with distilled water to the concentrations required for the experiments (0.5 mg mL^{-1} , 2.5 mg mL^{-1} , 5 mg mL^{-1} , 10 mg mL^{-1} and 20 mg mL^{-1}). Diluted solutions were heated in boiling water bath for 10 min, 20 min, 30 min (TTC30), 40 min, 50 min and 60 min (TTC60) to obtain the TTC. Absorbance of TTC were measured at 450 nm by a microplate reader. DFC was diluted with physiological saline to a concentration of $200 \text{ }\mu\text{g mL}^{-1}$ and heated in boiling water for 60 min (DFC60).

2.3 Cell culture conditions

Human normal liver cell LO2 cells (American Type Culture Collection, ATCC), human embryonic kidney cells 293 cells (ATCC), human embryonic lung diploid MRC-5 cells (ATCC), Mouse renal tubular epithelial cells (mTEC) were purchased from the China Cell Line Bank (Beijing, China) and cultured in RPMI 1640, DMEM, MEM and RPMI 1640 containing 10% FBS and 1% penicillin-streptomycin, respectively. Cells were cultured in a humidified incubator at 37°C with 5% CO_2 .

2.4 Cytotoxicity assays

Cytotoxicity was detected by the CCK-8 method according to the manufacturer's instructions. Briefly, LO2 cells, 293 cells or MRC-5 cells was seeded at a density of 1.0×10^4 , 1.0×10^4 or 5.0×10^3 cells per well in the 96-well plates, respectively. After cultured overnight, CEF or TTC was added to the wells ($10 \text{ }\mu\text{L}$ per well) to make the final concentration of each well equal to $125 \text{ }\mu\text{g mL}^{-1}$, $250 \text{ }\mu\text{g mL}^{-1}$, $500 \text{ }\mu\text{g mL}^{-1}$ or $1000 \text{ }\mu\text{g mL}^{-1}$, respectively. The wells without CEF and TTC were served as control group. After 24 h, 48 h or 72 h of treatment, the culture medium in the wells was aspirated and the cells were washed gently twice with PBS. CCK-8 ($10 \text{ }\mu\text{L}$ per well) and culture medium ($100 \text{ }\mu\text{L}$ per well) were added to the wells, and followed with an incubation from 1 h to 1.5 h (based on the different cell lines and cell intensity) at 37°C . Absorbance was measured at 450 nm by a microplate reader. The IC_{50} values at the different time points of 24 h, 48 h and 72 h were calculated according to the obtained OD values.^{40,41} The cell inhibition rate (%) was calculated by the following formula described by the manufacturers:

$$(\text{OD}_{\text{control}} - \text{OD}_{\text{test}} / \text{OD}_{\text{control}} - \text{OD}_{\text{blank}}) \times 100\%$$

where OD_{test} is the absorbance of the test wells, $\text{OD}_{\text{control}}$ represents the absorbance of the control wells, and OD_{blank} is the absorbance of the well containing just culture medium and CCK-8.

2.5 Assessment of nuclear morphological changes by Hoechst 33342/PI staining

LO2 cells were seeded in 48-well plates with round coverslips at a density of 2.0×10^4 cells per well. After cultured overnight, CEF or TTC30 was added to the wells to make the concentration to $1000 \text{ }\mu\text{g mL}^{-1}$. After incubation for 24 h, cells were gently washed three times with cold PBS, and resuspended with 1 mL of PBS. Then $5 \text{ }\mu\text{L}$ of Hoechst 33342 stain and $5 \text{ }\mu\text{L}$ of PI stain were added to each well, and followed with a dark incubation at 37°C for 20 min. After the dark incubation, the cells were washed once with PBS. Fluorescence microscopy was used to observe the morphological changes of the nucleus (Olympus).

2.6 Analysis of cell death by flow cytometry

The cell death of LO2 cells caused by TTC was identified using Annexin V-FITC/PI dyes and quantified through flow cytometry method. Cells were placed in 6-well plates at a density of 1×10^6 cells per well and cultured overnight. CEF, TTC30 or TTC60 was added to the wells to make the concentration to $1000 \text{ }\mu\text{g mL}^{-1}$. Cells were collected and resuspended in $500 \text{ }\mu\text{L}$ detection buffer, and then stained with $5 \text{ }\mu\text{L}$ Annexin V-FITC and $5 \text{ }\mu\text{L}$ PI dyes based on the manufacturer's instructions.⁴² Samples were quantified by using a flow cytometer (BD, C6) within 1 h.

2.7 LC-MS analysis

Five microliters of the samples ($500 \text{ }\mu\text{g mL}^{-1}$ of CEF, TTC30 and TTC60, $200 \text{ }\mu\text{g mL}^{-1}$ of DFC) were injected onto an Agilent1290 HPLC. The analytical column was a reversed-phase C18 column (ZORBAX, $2.1 \times 50 \text{ mm}$, $1.8 \text{ }\mu\text{m}$). A binary gradient with a flow rate of 0.7 mL min^{-1} was used in the tests. 0.1% formic acid (v/v) in water was used as mobile phase A, and 0.1% formic acid (v/v) in acetonitrile was used as mobile phase B.⁴³ The gradient started with 5% mobile phase B for 0.5 min, increased to 50% B from 0.5–5.0 min, to 95% B from 5.0–6.0 min. All target compounds were eluted out of the column within 6 min. Triple injections were made for each sample.

The mass spectrometry (MS) measurements were carried out on a Bruker microTOF-Q II equipped with an electrospray ionization (ESI) source operating in Auto-MSⁿ mode to obtain fragment ions. Analyses were performed in positive mode for all target compounds. The scanned range was the m/z 50–1500 Da in high sensitivity mode. The dry gas heater was 200°C and dry gas flow was 5.0 L min^{-1} . The nebulizer pressure was 0.4 bar and capillary was 4500 V. The collision cell RF was 100.0 Vpp.

2.8 Synthesis and cytotoxicity assay of CEF-1

The synthetic route and structural identification results were shown in the ESI (Fig. S1†). Synthesized CEF-1 was dissolved in DMSO to prepare a stock solution with a concentration of



400 mg mL⁻¹ and kept in the dark at -20 °C. LO2 cells were plated at a density of 1.0×10^4 cells per well in 96-well plates and cultured overnight. CEF-1 was added to wells to make the concentration of CEF-1 in each well equal to 0 $\mu\text{g mL}^{-1}$, 50 $\mu\text{g mL}^{-1}$, 100 $\mu\text{g mL}^{-1}$, 200 $\mu\text{g mL}^{-1}$ or 400 $\mu\text{g mL}^{-1}$, respectively, and followed an incubation of 24 h. After that, the inhibition rate or IC₅₀ value was calculated with the CCK-8 method as described above. The combined effect between CEF and CEF-1 was calculated by the Jin's formula. The Jin's formula was described as follows: $Q = Ea + b/(Ea + Eb - Ea \times Eb)$, where $Ea + b$, Ea and Eb are the average effects of TTC30, CEF, CEF-1, respectively. In this method, $Q < 0.85$ indicates antagonism, $0.85 \leq Q < 1.15$ indicates additivity, and $Q \geq 1.15$ indicates synergism.⁴⁴

Furthermore, mitochondrial transmembrane potential of LO2 cells treated with CEF-1 was evaluated. LO2 cells were seeded in 6-well plates at a density of 1×10^6 cells per well and cultured overnight. CEF-1 was added to wells (final concentrations: 0 $\mu\text{g mL}^{-1}$, 100 $\mu\text{g mL}^{-1}$, 200 $\mu\text{g mL}^{-1}$ and 400 $\mu\text{g mL}^{-1}$). Then, cells were incubated for 24 h. After incubation, cells were washed twice with PBS and incubated with JC-1 solution (10 $\mu\text{g mL}^{-1}$) for 20 min in the cell incubator. Fluorescent images of the LO2 cells were taken under a fluorescent microscope. The maximum excitation wavelength of JC-1 monomers was 514 nm and the maximum emission wavelength was 529 nm. The maximum excitation wavelength of JC-1 aggregates was 585 nm and the maximum emission wavelength is 590 nm. In addition, the inhibition rates of CEF, TTC60 and CEF-1 on mTEC cells (seeded at a density of 5.0×10^3 cells per well in the 96-well plates) for 72 h were calculated through CCK-8 method.

2.9 Statistical analyses

Statistics were analyzed using the GraphPad Prism 5 program. Data were shown as the means \pm SD. Student's *t*-test analysis method was used to determine statistical significance (group = 2). Other significant differences were analyzed by one-way ANOVA followed by Dunnett's *t* test or Newman-Keuls test (group ≥ 3). $p < 0.05$ were considered statistically significant.

3. Results

3.1 Composition of CEF changed after thermal treatment

The color changes of CEF and TTC at concentration of 20 mg mL⁻¹ were shown in Fig. 1A. These results indicated that the color of the solution gradually became darker. Based on this phenomenon, we speculated that the composition of TTC was different from CEF. In Fig. 1B, the absorbance values of CEF and TTC at different concentration (2.5 mg mL⁻¹, 5.0 mg mL⁻¹, 10 mg mL⁻¹ and 20 mg mL⁻¹) were raised with the thermal time increased. Besides, the slopes of absorbance at 30 min were greater than 10 min and 20 min, and the slopes of the absorbance for 60 min were greater than 40 min and 50 min. These results indicated that the composition change were more obviously at these two time points (30 min and 60 min).

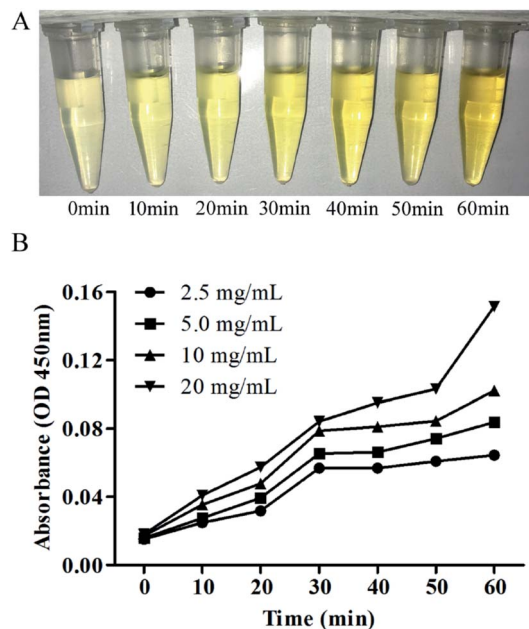


Fig. 1 The color and absorbance values of CEF and TTC. (A) The color of CEF was varied for the different heating time (0 min, 10 min, 20 min, 30 min, 40 min, 50 min and 60 min) at concentration of 20 mg mL⁻¹. (B) The absorbance value of different concentrations of CEF and TTC at 450 nm (2.5 mg mL⁻¹, 5.0 mg mL⁻¹, 10 mg mL⁻¹ and 20 mg mL⁻¹). Data are expressed as the mean from three independent experiments.

3.2 TTC inhibited cell proliferation

Cell proliferation inhibition assays were employed to study the effect of TTC on cells. Fig. 2A showed that at concentration of 1000 $\mu\text{g mL}^{-1}$, TTC inhibited the proliferation of LO2 cells and the inhibition effect was heating time dependent. Moreover, the toxicity of TTC30 was significantly higher than CEF at all three time points (24 h, 48 h, 72 h incubation), and the toxicity of TTC60 was further increased. Therefore, combined with results in Fig. 1B, these two thermal time points (30 min and 60 min) were used for subsequent toxicity studies.

Based on the cytotoxicity of TTC described above, we further investigated the cytotoxicity of TTC30 at different concentrations (125 $\mu\text{g mL}^{-1}$, 250 $\mu\text{g mL}^{-1}$, 500 $\mu\text{g mL}^{-1}$, 1000 $\mu\text{g mL}^{-1}$) and different treating times (24 h, 48 h, 72 h) on LO2 cells. These results revealed that the cytotoxicity of TTC30 was significantly higher than that of CEF at same concentration. Moreover, the cytotoxicity presented a dose- and time-dependent manner (Fig. 2B–D). The IC₅₀ values of CEF and TTC30 decreased with incubation time increased (from 24 h to 72 h), and the IC₅₀ value of TTC30 was significantly lower than that of CEF at each time point (Fig. 2E). In addition, similar results were obtained by using TTC30 to treat 293 cells (Fig. 2F) or MRC-5 cells (Fig. 2G). IC₅₀ comparison of three cell lines at 72 hours was shown in Fig. 2H.

3.3 TTC induced cell apoptosis

Fluorescence microscopy and flow cytometry assays were performed to further investigate the cytotoxicity of TTC30 on LO2 cells. As shown in Fig. 3, early apoptosis event was observed in LO2

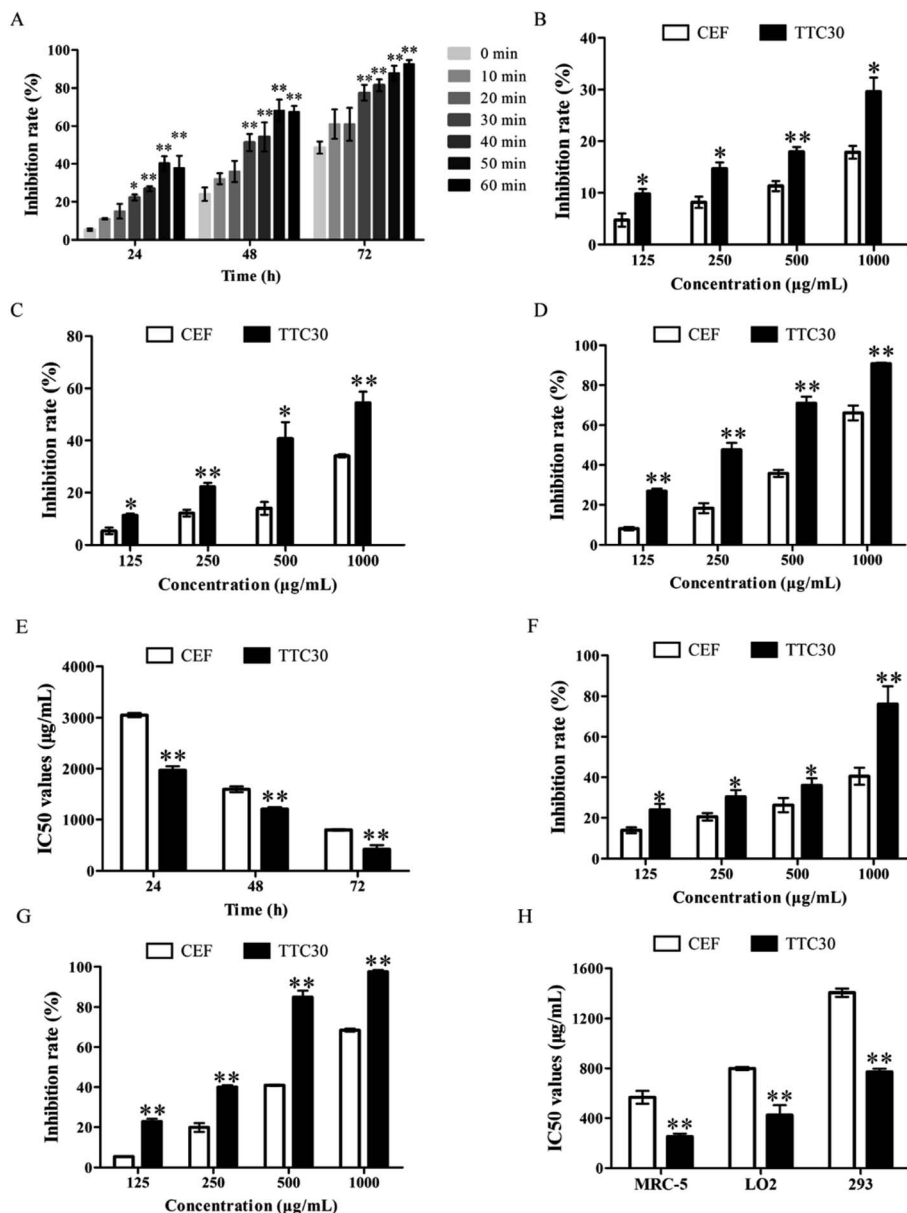


Fig. 2 The inhibition rates and IC₅₀ values of CEF and TTC on LO2 cells, 293 cells and MRC-5 cells. (A) The inhibition rate of CEF and TTC at concentration of 1000 $\mu\text{g mL}^{-1}$ on LO2 cells. The cell inhibition rate was calculated according to the data detected using the CCK-8 method. Data are expressed as the mean \pm SD from three independent experiments, and significant differences were analyzed by one-way ANOVA followed by a Dunnett's *t* test. **p* < 0.05 or ***p* < 0.01 compared with the 0 min group. (B) The inhibition rate of CEF and TTC30 on LO2 cells. LO2 cells were treated with different concentrations (125 $\mu\text{g mL}^{-1}$, 250 $\mu\text{g mL}^{-1}$, 500 $\mu\text{g mL}^{-1}$ and 1000 $\mu\text{g mL}^{-1}$) of TTC30 for 24 h, (C) 48 h, and (D) 72 h. (E) The IC₅₀ values of CEF and CHP30 on LO2 cells after treatment for 24 h, 48 h and 72 h. (F) The inhibition rate of CEF and TTC30 on 293 cells and MRC-5 cells (G), 293 cells and MRC-5 cells were treated with different concentrations (125 $\mu\text{g mL}^{-1}$, 250 $\mu\text{g mL}^{-1}$, 500 $\mu\text{g mL}^{-1}$ or 1000 $\mu\text{g mL}^{-1}$) of TTC30 for 72 h. (H) The comparison of the IC₅₀ values in MRC-5 cells, LO2 cells and 293 cells after TTC30 treatment for 72 h. The cell inhibition rate was calculated according to the data detected using the CCK-8 method. Data are expressed as the mean \pm SD from three independent experiments. **p* < 0.05 or ***p* < 0.01 compared with the CEF group using *t*-test analysis.

cells (showed blue fluorescence, yellow arrow) when treated with 1000 $\mu\text{g mL}^{-1}$ of TTC30 or TTC60. Furthermore, late apoptosis event was also observed (cells showed both red fluorescence and blue fluorescence, white arrow). These results indicated that TTC induced cytotoxicity by causing cell apoptosis.

In the flow cytometry assays, the percent of apoptotic cells in the TTC30 or TTC60 groups was significant higher than that in

the control group, demonstrating that TTC could induce LO2 cell apoptosis (Fig. 4).

3.4 Analysis of toxic components in TTC

HPLC-TOF-MS method was employed to analyze the components of TTC. The extracted ion chromatogram (EIC) of CEF, TTC30 and TTC60 were depicted in Fig. 5A. The EIC of CEF



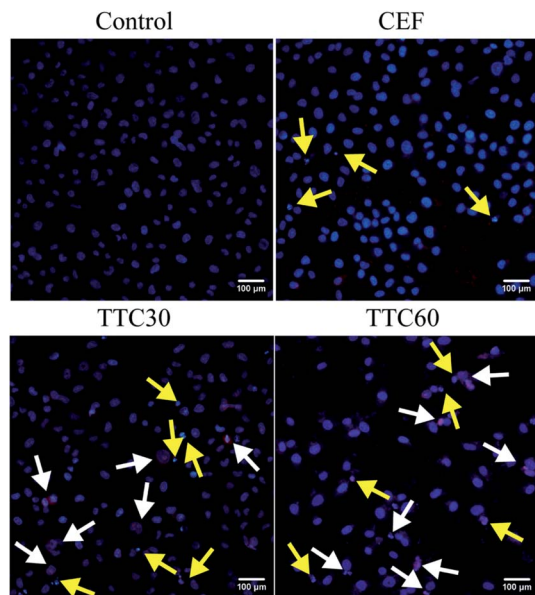


Fig. 3 Fluorescence observation of LO2 cells stained by Hoechst 33342 and PI after treatment with concentrations of $1000 \mu\text{g mL}^{-1}$ of CEF or TTC30 for 24 h; $200\times$ magnification. The chromatin shrunk (yellow arrow) and the nucleus fragmented (white arrow).

showed one peak at a retention time (RT) of 2.9 min. Both the EIC of TTC30 and TTC60 exhibited two peaks at RT of 0.4 min and 2.9 min. The different chromatographic results between CEF and TTC revealed that a new compound (named CEF-1 in this paper) appeared during thermal treatment of CEF. By calculating from the peak area of the EIC, the relative amount of CEF-1 in TTC 30 or TTC60 was approximately 10.03% and 12.20%, respectively (Table 1), indicating that the amount of

CEF-1 was increased with heating time. Besides, the CEF did not decompose completely at this heating condition.

CEF was observed at a retention time of 2.9 min with a molecular ion peak at m/z 524.0 (Fig. 5B). The peak at m/z 241.0 was assigned to the cleavage of the β -lactam ring of CEF as a fragment ion. CEF was confirmed by the precursor ion (m/z) of 524.0 and fragment ion (m/z) of 241.0 which was consistent with an authentic standard and a previous report.⁴⁵ In the spectrum of both TTC30 and TTC60, m/z 243.1 was considered to be the molecular ion (Fig. 5C). The structure of this molecular ion was considered to be the aldehyde resulting from the cleavage of the β -lactam ring^{43,46} (CEF-aldehyde or CEF-1 in this paper). The chemical structural formula of CEF-1 and route of generation from CEF were shown in Fig. 5D. In addition, we also detected the DFC, the primary metabolites of CEF, after heating for 60 min by LC-MS method to investigate the presence of CEF-1 in thermal treatment DFC. In Fig. 5E, a peak was observed at RT of 0.4 min. Furthermore, we confirmed the compound of this peak showed a molecular ion peak at m/z 243.1 and a main fragment ion peak at m/z 126.0 by LC-MS method, which was consistent with CEF-1.

3.5 CEF-1 inhibited the proliferation of LO2 cells and mTEC cells

The synthesis route of CEF-1 was shown in ESI (Fig. S1A†). Synthesized CEF-1 was showed in Fig. S1B† and identified by MS (Fig. S1C†). The inhibition effect of CEF-1 on LO2 cells was determined by the CCK-8 method described above. As shown in Fig. 6A, CEF-1 significantly inhibited cell proliferation in a dose-dependent manner. Jin's formula was used to investigate the effect of CEF combined with CEF-1 on LO2 cells and the Q value was 0.8938, demonstrating that CEF and CEF-1 had an additive

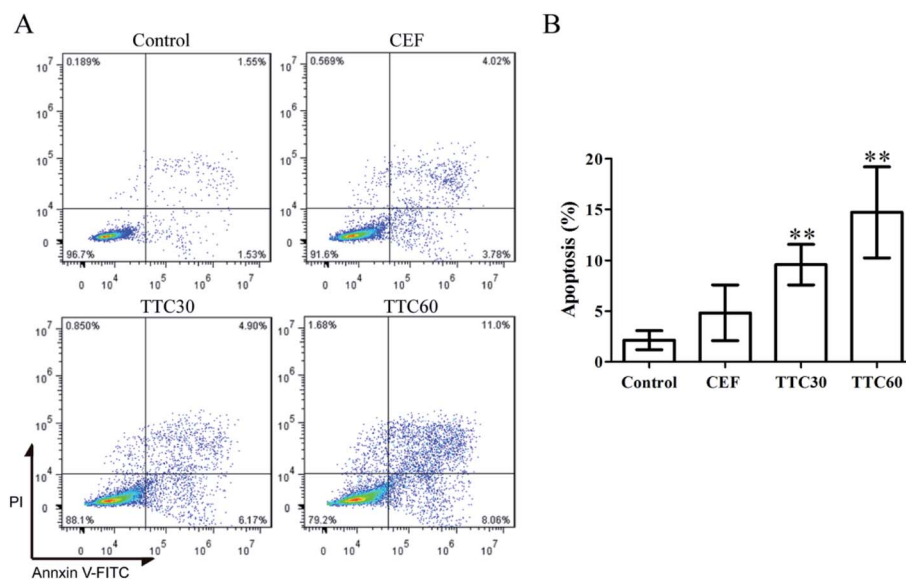


Fig. 4 Flow cytometry analysis of LO2 cells treated with concentration of $1000 \mu\text{g mL}^{-1}$ of CEF, TTC30 or TTC60 for 24 h using FITC-Annexin V/PI staining. (A) Cells were stained with Annexin V-FITC/PI dyes at room temperature for 15 min in the dark and analyzed by using flow cytometry. (B) Quantity of apoptosis rates for LO2 cells based on the flow cytometry assay results. Data are expressed as the mean \pm SD from three independent experiments. * $p < 0.05$ or ** $p < 0.01$ compared with the control group using t -test analysis.



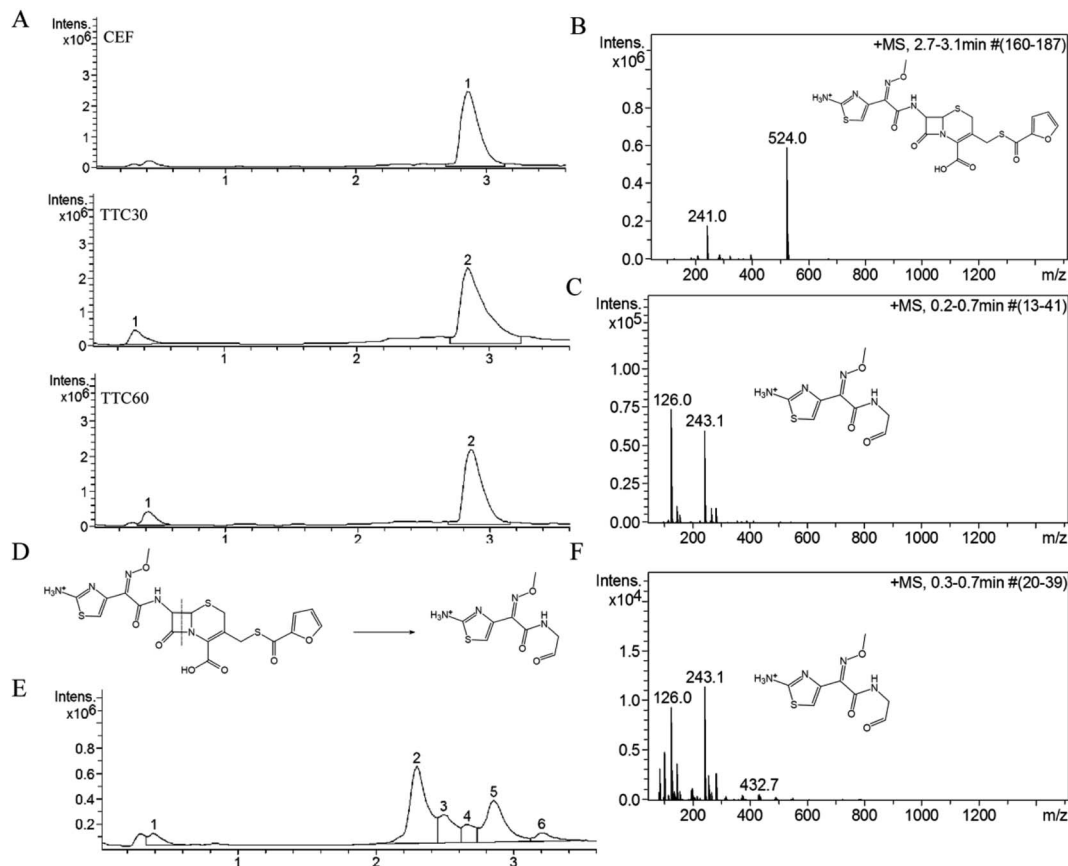


Fig. 5 CEF-aldehyde (CEF-1) was one of degradation products of thermally treated CEF or DFC. (A) The extracted ion chromatogram (EIC) of CEF, TTC30 and TTC60, respectively. (B) Mass spectrometry (MS) analysis results of the peak at RT 2.9 min of CEF, TTC30 and TTC60. (C) MS analysis results of the peak at RT 0.4 min of TTC30 and TTC60. (D) The route of generation of CEF-1 from CEF. (E) The EIC of DFC60. (F) MS analysis result of the peak at RT 0.4 min of DFC60.

Table 1 Retention time (min), molecular weight (m/z) and relatively area (%) of CEF, TTC30, TTC60 and DFC60

	Peak	RT (min)	Molecular weight (m/z)	Relatively area (%)
CEF	1	2.9	524.0	100
TTC30	1	0.4	243.1	10.03
	2	2.9	524.0	89.97
TTC60	1	0.4	243.1	12.20
	2	2.9	524.0	87.80
DFC60	1	0.4	243.1	6.64
	2	2.3	412.0	46.69
	3	2.5	386.0	16.64
	4	2.7	558.0	8.72
	5	2.9	186.2	29.22
	6	3.2	337.2	5.38
	7	5.2	430.9	15.95

cytotoxicity. The result indicated that the cytotoxicity of TTC30 was caused by the addition of CEF-1 generated from CEF degradation and incompletely decomposed CEF, that is to say, the main toxic compound produced after heating of CEF was CEF-1. We further calculated the IC_{50} values of CEF, TTC30 and

CEF-1 at 24 h on LO2 cells (Fig. 6B). The IC_{50} value of CEF-1 was $573.1 \mu\text{g mL}^{-1}$ which was approximately 5.3 times lower than CEF ($3052.0 \mu\text{g mL}^{-1}$) and 3.4 times lower than TTC30 ($1967.0 \mu\text{g mL}^{-1}$). JC-1 staining is a method to identified the mitochondrial transmembrane potential. Mitochondrial membrane potential of healthy cells showed red fluorescence. When cells underwent apoptosis, mitochondrial membrane potential produced green fluorescence. As Fig. 6C showed, cells treated with CEF-1 produced more green fluorescence than control. Thus, CEF-1 could reduced mitochondrial membrane potential of LO2 cells, indicating that CEF-1 could cause cell apoptosis. In addition, CEF-1 exhibited significant cytotoxicity on mTEC cells compared with CEF and TTC60 (Fig. 6D). All these results demonstrated that CEF-1 was the main toxic thermal degradation product of CEF.

4. Discussion

CEF is an unstable antibiotic that is sensitive to temperature, pH and light.^{35–39,47–50} Due to the high ring strain of the small β -lactone ring, the degradation was temperature- and time-dependent according to previous studies.^{34,37,43,51} In the study by Junza *et al.*, CEF-1 was the only one degradation



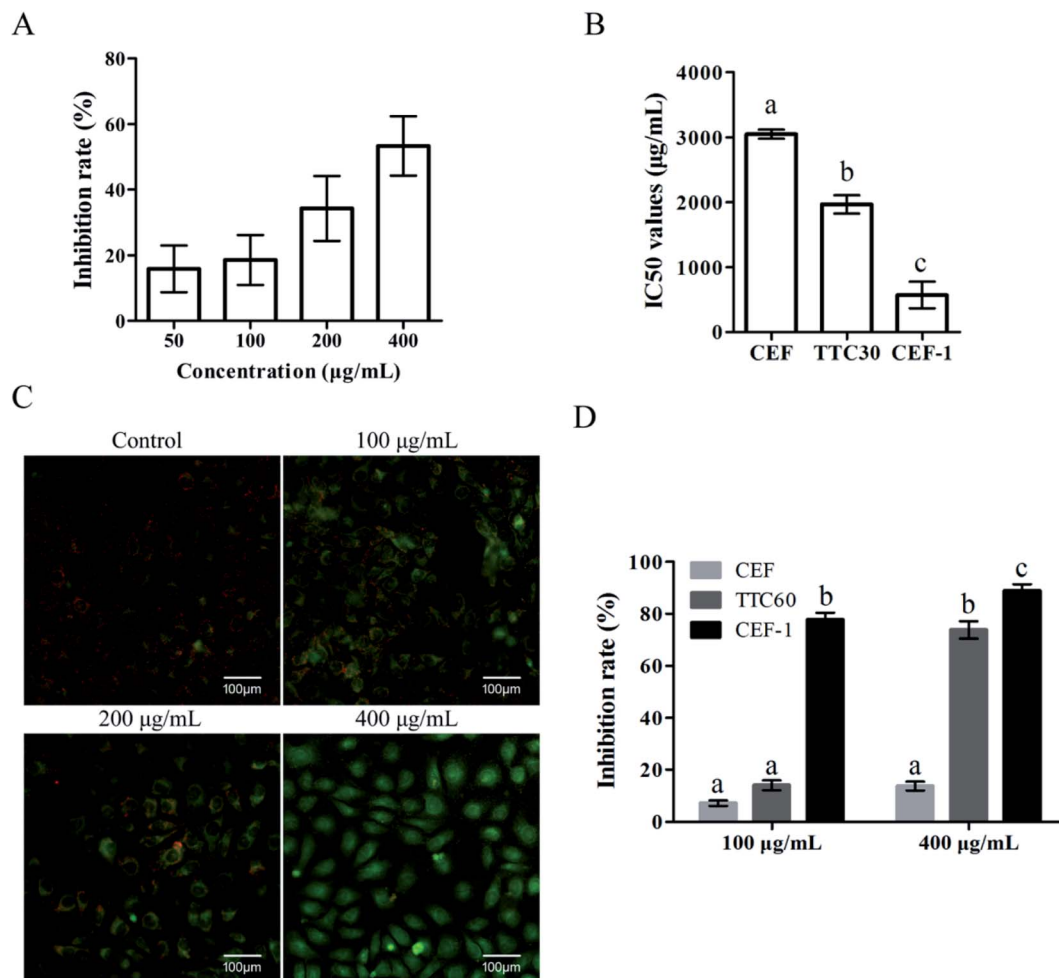


Fig. 6 The effect of CEF-1 on LO2 cells and mTEC cells. (A) LO2 cells were treated with CEF-1 at concentrations of 50 $\mu\text{g mL}^{-1}$, 100 $\mu\text{g mL}^{-1}$, 200 $\mu\text{g mL}^{-1}$ or 400 $\mu\text{g mL}^{-1}$ for 24 h. (B) Comparison of the IC₅₀ values after 24 h of treatment among CEF, TTC30 and CEF-1. (C) Fluorescence observation of LO2 cells stained by JC-1 after treatment with CEF-1 at concentrations of 100 $\mu\text{g mL}^{-1}$, 200 $\mu\text{g mL}^{-1}$ and 400 $\mu\text{g mL}^{-1}$ for 24 h; 200 \times magnification. (D) mTEC cells were treated with CEF, TTC60 and CEF-1 at concentrations of 100 $\mu\text{g mL}^{-1}$ and 400 $\mu\text{g mL}^{-1}$ for 72 h. Cell inhibition rates were calculated according to the data detected using the CCK-8 method. Data are expressed as the mean \pm SD from three independent experiments, and significant differences were analyzed by one-way ANOVA followed by a Newman–Keuls test. Different letters indicate significant difference between groups ($p < 0.05$).

product of CEF at low concentration of 2 $\mu\text{g mL}^{-1}$ heated for 30 min at 120 $^{\circ}\text{C}$ both in water and in milk environment.⁴³ Our study suggested that CEF-1 was the main degradation product after heating at 100 $^{\circ}\text{C}$ for 30 min and 60 min, which was similar to the previous research results.⁴³ It was suggested that the main degradation mechanism of CEF at high temperature was the cleavage of the β -lactam ring. Previous studies showed that the degradation pathways of cephalosporins in the environment were abiotic hydrolysis, photodegradation and biodegradation.^{47,48,52} CEF-1 was the main biodegradation product of CEF and the biodegradation could increase the ecotoxicity.^{36,49} According to X. Li *et al.*, the optimum temperature range of CEF-1 for biodegradation was between 25 $^{\circ}\text{C}$ and 45 $^{\circ}\text{C}$,³⁶ which is similar to the temperature for cheese fermentation.^{53–57}

During food processing, whether through industrialization or at home, the temperature is usually higher than 50 $^{\circ}\text{C}$.^{58,59}

The high cooking temperature can kill the pathogen to ensure food hygiene, longer shelflife, safety and/or better taste.^{60,61} For example, the industrial sterilization temperature for infant/intestine formulations is usually higher than 110 $^{\circ}\text{C}$ lasting 20–30 min.⁶² Therefore, in the process of food production and processing, the conditions are met for the generation of CEF-1. DFC is known as the main metabolite of CEF *in vivo* and is regarded as the residue of CEF in meat, milk and other tissues.^{63,64} Our experimental results proved that CEF-1 also appeared from the degradation of DFC, indicating that CEF-1 may be present in CEF residual food productions. Here, we verified that thermally treated CEF showed increased cytotoxicity on human liver, lung and kidney cells *in vitro*. These cell lines represented organs rich in blood vessels which were easily damaged by intake of toxic compound. Furthermore, the cytotoxicity experiments performed by the synthesis CEF-1 verified

that CEF-1 was the main toxic compound in thermally treated CEF.

Ying Shao *et al.* reported that Na₂S (a known toxicity compound as a soluble sulfide donor) showed cytotoxicity in LO2 cells at concentrations above 0.1 mM and the inhibition rate of sulfide for 24 h at concentration of 1 mM was almost 82.50%.⁶⁵ In our study, the inhibition rate of CEF-1 at concentration of 1 mM was approximately 35.36%, which was calculated according to results of cytotoxicity tests, demonstrating that the cytotoxicity induced by CEF-1 nearly was 2.33-fold lower than that induced by Na₂S. Besides, dichloroacetonitrile is a kind of disinfection by products of water chlorination, which could induce cytotoxicity by apoptosis in LO2 cells. The viability rate of dichloroacetonitrile for 24 h at concentration of 100 µM was 78.92%.⁶⁶ Our data showed that the viability rate of CEF-1 for 24 h at concentration of 100 µg mL⁻¹ (approximately equal to 412 µM) was 81.39% (Fig. 6A), indicating that the cytotoxicity induced by CEF-1 nearly was 4-fold lower than that induced by dichloroacetonitrile. Previous studies in our laboratory also confirmed that penicillin, another β-lactam antibiotic, posed a public health risk after cooking.^{41,67} Considering the cytotoxicity of CEF-1, we should strengthen the detection of CEF or DFC in food.

To date, HPLC and LC-MS are the main methods to analyze the residual conditions of CEF in tissues or other productions. However, these two methods include extraction and the SPE process by using alkaline solutions which could lead to CEF degradation.³⁹ Tissue processing and sampling without suitable precautions could lead to the lower detection levels than actual existence, which may cause the neglect of the threat posed by residual CEF or DFC in tissues since the cytotoxicity of CEF-1. Thus, in consideration of the instability of CEF, CEF-1 might have the potential as a marker of CEF detection in animal-derived foods.

5. Conclusion

Our data indicated that CEF-aldehyde, the main CEF thermal degradation product, could cause cytotoxicity by inducing apoptosis. Moreover, we detected CEF-aldehyde in thermally treated DFC, the main metabolite of CEF in animals. To our knowledge, this is the first report on the cytotoxicity of thermally treated CEF, which is meaningful for food safety and public health.

Abbreviations

CEF	Ceftiofur
TTC	Thermally treated CEF
LC-MS	Liquid chromatography-mass spectrometry
CEF-1	CEF-aldehyde
DFC	Desfuoylceftiofur
IMM	Intramammary
FBS	Fetal bovine serum
RPIM 1640 medium	Roswell park memorial institute 1640 medium

DMEM	Dulbecco's modified eagle medium
MEM	Eagle's minimum essential medium
ESI	Electrospray ionization
EIC	Extracted ion chromatogram
RT	Retention time

Conflicts of interest

The authors declare they have no actual or potential competing financial interests.

Acknowledgements

This work was financially supported by grants from the National Key Research and Development Program of China (No. 2018YFD0500504) and the National Natural Science Foundation of Jilin Province, P. R. China (Grant No. 20170101035JC).

References

- 1 T. P. Van Boeckel, C. Brower, M. Gilbert, B. T. Grenfell, S. A. Levin, T. P. Robinson, A. Teillant and R. Laxminarayan, Global trends in antimicrobial use in food animals, *Proc. Natl. Acad. Sci. U. S. A.*, 2015, **112**, 5649–5654.
- 2 A. G. Mathew, R. Cissell and S. Liamthong, Antibiotic resistance in bacteria associated with food animals: A United States perspective of livestock production, *Foodborne Pathog. Dis.*, 2007, **4**, 115–133.
- 3 T. P. Van Boeckel, E. E. Glennon, D. Chen, M. Gilbert, T. P. Robinson, B. T. Grenfell, S. A. Levin, S. Bonhoeffer and R. Laxminarayan, Reducing antimicrobial use in food animals Consider user fees and regulatory caps on veterinary use, *Science*, 2017, **357**, 1350–1352.
- 4 C. Kirchhelle, Pharming animals: a global history of antibiotics in food production (1935–2017), *Palgrave Commun.*, 2018, **4**.
- 5 J. Chen, G. G. YingW and J. Deng, Antibiotic Residues in Food: Extraction, Analysis, and Human Health Concerns, *J. Agric. Food Chem.*, 2019, **67**, 7569–7586.
- 6 K. T. KoshyA and R. Cazars, Controlled hydrolysis of ceftiofur sodium, a broad-spectrum cephalosporin; isolation and identification of hydrolysis products, *J. Pharm. Sci.*, 1997, **86**, 389–395.
- 7 C. S. Aaron, R. L. Yu, P. R. Harbach, J. M. Mazurek, D. H. Swenson, D. Kirkland, R. Marshall and S. McEnaney, Comparative mutagenicity testing of ceftiofur sodium: I. Positive results in *in vitro* cytogenetics, *Mutat. Res.*, 1995, **345**, 27–35.
- 8 C. S. Aaron, R. L. Yu, J. A. Bacon, D. Kirkland, S. McEnaney and R. Marshall, Comparative mutagenicity testing of ceftiofur sodium. II. Cytogenetic damage induced *in vitro* by ceftiofur is reversible and is due to cell cycle delay, *Mutat. Res.*, 1995, **345**, 37–47.
- 9 C. S. Aaron, R. L. Yu, P. S. Jaglan, R. D. Roof, C. Hamilton, R. Sorg, R. Gudi and A. Thilagar, Comparative



- mutagenicity testing of ceftiofur sodium: III. Ceftiofur sodium is not an *in vivo* clastogen, *Mutat. Res.*, 1995, **345**, 49–56.
- 10 Zoetis, *NAXCEL® (CEFTIOFUR SODIUM) sterile powder*, https://www.zoetisus.com/products/pork/naxcel_ceftiofur-sodium-sterile-powder.aspx.
 - 11 D. M. Foster, M. E. Jacob, K. A. Farmer, B. J. Callahan, C. M. Theriot, S. Kathariou, N. Cernicchiaro, T. PrangeM and G. Papich, Ceftiofur formulation differentially affects the intestinal drug concentration, resistance of fecal *Escherichia coli*, and the microbiome of steers, *PLoS One*, 2019, **14**, e0223378.
 - 12 M. Apley, Bovine respiratory disease: pathogenesis, clinical signs, and treatment in lightweight calves, *Vet. Clin. Food Anim. Pract.*, 2006, **22**, 399–411.
 - 13 S. C. Donaldson, B. A. Straley, N. V. Hegde, A. A. Sawant, C. DebRoyB and M. Jayarao, Molecular epidemiology of ceftiofur-resistant *Escherichia coli* isolates from dairy calves, *Appl. Environ. Microbiol.*, 2006, **72**, 3940–3948.
 - 14 A. Espadamala, R. Pereira, P. Pallares, A. Lago and N. Silva-Del-Rio, Metritis diagnosis and treatment practices in 45 dairy farms in California, *J. Dairy Sci.*, 2018, **101**, 9608–9616.
 - 15 S. E. IvesJ and T. Richeson, Use of Antimicrobial Metaphylaxis for the Control of Bovine Respiratory Disease in High-Risk Cattle, *Vet. Clin. Food Anim. Pract.*, 2015, **31**, 341–350.
 - 16 E. Fernandez-Varon, C. Carceles-Garcia, J. M. Serrano-RodriguezC and M. Carceles-Rodriguez, Pharmacokinetics (PK), pharmacodynamics (PD), and PK-PD integration of ceftiofur after a single intravenous, subcutaneous and subcutaneous-LA administration in lactating goats, *BMC Vet. Res.*, 2016, **12**, 232.
 - 17 G. S. Waraich, P. K. Sidhu, P. S. Daundkar, G. KaurS and K. Sharma, Pharmacokinetic and pharmacodynamic characterization of ceftiofur crystalline-free acid following subcutaneous administration in domestic goats, *J. Vet. Pharmacol. Ther.*, 2017, **40**, 429–438.
 - 18 D. F. Alba, G. da Rosa, D. Hanauer, T. F. Saldanha, C. F. Souza, M. D. Baldissera, D. da Silva Dos Santos, A. P. Piovezan, L. K. Girardini and A. Schafer Da Silva, Subclinical mastitis in Lacaune sheep: causative agents, impacts on milk production, milk quality, oxidative profiles and treatment efficacy of ceftiofur, *Microb. Pathog.*, 2019, **137**, 103732.
 - 19 A. C. B. Berge, W. M. SischoA and L. Craigmill, Antimicrobial susceptibility patterns of respiratory tract pathogens from sheep and goats, *J. Am. Vet. Med. Assoc.*, 2006, **229**, 1279–1281.
 - 20 M. D. Barton, Impact of antibiotic use in the swine industry, *Curr. Opin. Microbiol.*, 2014, **19**, 9–15.
 - 21 M. Zeineldin, A. Megahed, B. Burton, B. Blair, B. Aldridge and J. F. Lowe, Effect of Single Dose of Antimicrobial Administration at Birth on Fecal Microbiota Development and Prevalence of Antimicrobial Resistance Genes in Piglets, *Front. Microbiol.*, 2019, **10**, 1414.
 - 22 R. Edirmanasinghe, R. Finley, E. J. Parmley, B. P. Avery, C. Carson, S. Bekal, G. Golding and M. R. Mulvey, A Whole-Genome Sequencing Approach To Study Cefoxitin-Resistant *Salmonella enterica* Serovar Heidelberg Isolates from Various Sources, *Antimicrob. Agents Chemother.*, 2017, **61**, e01919-16.
 - 23 R. E. Hornish and S. F. Kotarski, Cephalosporins in veterinary medicine - ceftiofur use in food animals, *Curr. Top. Med. Chem.*, 2002, **2**, 717–731.
 - 24 USDA, *Milk quality, milking procedures, and mastitis on U.S. dairies*, USDA-Animal and Plant Health Inspection Service-Veterinary Services, National Animal Health Monitoring System, Riverdale, MD, 2014, https://www.aphis.usda.gov/animal_health/nahms/dairy/downloads/dairy14/Dairy14_dr_Mastitis.pdf, accessed 2016.
 - 25 P. N. Tempini, S. S. Aly, B. M. KarleR and V. Pereira, Multidrug residues and antimicrobial resistance patterns in waste milk from dairy farms in Central California, *J. Dairy Sci.*, 2018, **101**, 8110–8122.
 - 26 E. K. Ganda, N. Gaeta, A. Sipka, B. Pomeroy, G. Oikonomou, Y. H. SchukkenR and C. Bicalho, Normal milk microbiome is reestablished following experimental infection with *Escherichia coli* independent of intramammary antibiotic treatment with a third-generation cephalosporin in bovines, *Microbiome*, 2017, **5**, 74.
 - 27 G. W. Smith, R. Gehring, J. E. Riviere, J. L. YeattsR and E. Baynes, Elimination kinetics of ceftiofur hydrochloride after intramammary administration in lactating dairy cows, *J. Am. Vet. Med. Assoc.*, 2004, **224**, 1827–1830.
 - 28 W. E. Owens, Z. Y. Xiang, C. H. Ray and S. C. Nickerson, Determination of milk and mammary tissue concentrations of ceftiofur after intramammary and intramuscular therapy, *J. Dairy Sci.*, 1990, **73**, 3449–3456.
 - 29 R. Han, S. Li, J. Wang, Z. Yu, J. Wang and N. Zheng, Elimination kinetics of ceftiofur hydrochloride in milk after an 8-day extended intramammary administration in healthy and infected cows, *PLoS One*, 2017, **12**, e0187261.
 - 30 Z. Lin, C. I. VahlJ and E. Riviere, Human Food Safety Implications of Variation in Food Animal Drug Metabolism, *Sci. Rep.*, 2016, **6**, 27907.
 - 31 USDA, *United States National Residue Program for Meat, Poultry, and Egg Products*, 2018, <https://www.fsis.usda.gov/wps/wcm/connect/d6badf7-0352-4a0e-a86d-32ba2d4613ba/2018-red-book.pdf?MOD=AJPERES>.
 - 32 S. E. KatzM and S. Brady, Antibiotic residues in food and their significance (Reprinted from *Antimicrobials in Foods*, pg 571–595, 1993), *Food Biotechnol.*, 2000, **14**, 147–171.
 - 33 L. Canton, L. Alvarez, C. Canton, L. Ceballos, C. Farias, C. Lanusse and L. Moreno, Effect of cooking on the stability of veterinary drug residues in chicken eggs, *Food Addit. Contam., Part A: Chem., Anal., Control, Exposure Risk Assess.*, 2019, **36**, 1055–1067.
 - 34 M. Roca, L. Villegas, M. L. Kortabitarte, R. L. AlthausM and P. Molina, Effect of heat treatments on stability of beta-lactams in milk, *J. Dairy Sci.*, 2011, **94**, 1155–1164.
 - 35 G. Sunkara, C. B. NavarreU and B. Kompella, Influence of pH and temperature on kinetics of ceftiofur degradation in aqueous solutions, *J. Pharm. Pharmacol.*, 1999, **51**, 249–255.



- 36 X. Li, W. Zheng, M. L. Machesky, S. R. Yates and M. Katterhenry, Degradation kinetics and mechanism of antibiotic ceftiofur in recycled water derived from a beef farm, *J. Agric. Food Chem.*, 2011, **59**, 10176–10181.
- 37 L. Tian, S. Khalil and S. Bayen, Effect of thermal treatments on the degradation of antibiotic residues in food, *Crit. Rev. Food Sci. Nutr.*, 2017, **57**, 3760–3770.
- 38 A. R. Ribeiro, H. V. LutzeT and C. Schmidt, Base-catalyzed hydrolysis and speciation-dependent photolysis of two cephalosporin antibiotics, ceftiofur and cefapirin, *Water Res.*, 2018, **134**, 253–260.
- 39 B. J. Berendsen, M. L. Essers, P. P. Mulder, G. D. van Bruchem, A. Lommen, W. M. van OverbeekL and A. Stolker, Newly identified degradation products of ceftiofur and cepapirin impact the analytical approach for quantitative analysis of kidney, *J. Chromatogr. A*, 2009, **1216**, 8177–8186.
- 40 J. L. Lou, G. H. Chu, G. J. Zhou, J. Jiang, F. F. Huang, J. J. Xu, S. Zheng, W. Jiang, Y. Z. Lu, X. X. Li, Z. J. ChenJ and L. He, Comparison between two kinds of cigarette smoke condensates (CSCs) of the cytogenotoxicity and protein expression in a human B-cell lymphoblastoid cell line using CCK-8 assay, comet assay and protein microarray, *Mutat. Res., Genet. Toxicol. Environ. Mutagen.*, 2010, **697**, 55–59.
- 41 C. Cui, H. J. Lu, Q. Hui, S. Y. Lu, Y. Liu, W. Ahmad, Y. Wang, P. Hu, X. L. Liu, Y. Cai, L. J. Liu, X. Zhang, K. Zhao, Y. S. Li, H. L. Ren, N. Y. JinZ and S. Liu, A preliminary investigation of the toxic effects of Benzylpenicilloic acid, *Food Chem. Toxicol.*, 2018, **111**, 567–577.
- 42 R. Yuan, H. L. Xu, X. H. Liu, Y. Tian, C. Li, X. L. Chen, S. A. Su, I. Perelshtein, A. Gedanken and X. K. Lin, Zinc-Doped Copper Oxide Nanocomposites Inhibit the Growth of Human Cancer Cells through Reactive Oxygen Species-Mediated NF-kappa B Activations, *ACS Appl. Mater. Interfaces*, 2016, **8**, 31806–31812.
- 43 A. Junza, A. Montane, J. Barbosa, C. Minguillon and D. Barron, High resolution mass spectrometry in the identification of transformation products and metabolites from beta-lactam antibiotics in thermally treated milk, *J. Chromatogr. A*, 2014, **1368**, 89–99.
- 44 L. Y. Jiang, M. Lian, H. Wang, J. G. Fang and Q. Wang, Inhibitory Effects of 5-Aza-2'-Deoxycytidine and Trichostatin A in Combination with p53-Expressing Adenovirus on Human Laryngocarcinoma Cells, *Chin. J. Cancer Res.*, 2012, **24**, 232–237.
- 45 L. Kantiani, M. Farre, M. Sibum, C. Postigo, M. L. de Alda and D. Barcelo, Fully Automated Analysis of beta-Lactams in Bovine Milk by Online Solid Phase Extraction-Liquid Chromatography-Electrospray-Tandem Mass Spectrometry, *Anal. Chem.*, 2009, **81**, 4285–4295.
- 46 X. L. Li, W. Zheng, M. L. Machesky, S. R. Yates and M. Katterhenry, Degradation Kinetics and Mechanism of Antibiotic Ceftiofur in Recycled Water Derived from a Beef Farm, *J. Agric. Food Chem.*, 2011, **59**, 10176–10181.
- 47 X. H. WangA and Y. Lin, Phototransformation of cephalosporin antibiotics in an aqueous environment results in higher toxicity, *Environ. Sci. Technol.*, 2012, **46**, 12417–12426.
- 48 M. Jiang, L. Wang and R. Ji, Biotic and abiotic degradation of four cephalosporin antibiotics in a lake surface water and sediment, *Chemosphere*, 2010, **80**, 1399–1405.
- 49 A. R. Ribeiro, B. Sures and T. C. Schmidt, Ecotoxicity of the two veterinarian antibiotics ceftiofur and cefapirin before and after photo-transformation, *Sci. Total Environ.*, 2018, **619**, 866–873.
- 50 A. R. Ribeiro and T. C. Schmidt, Determination of acid dissociation constants (pK(a)) of cephalosporin antibiotics: Computational and experimental approaches, *Chemosphere*, 2017, **169**, 524–533.
- 51 M. P. Hermo, P. Gomez-Rodriguez, J. Barbosa and D. Barron, Metabolomic assays of amoxicillin, cepapirin and ceftiofur in chicken muscle: Application to treated chicken samples by liquid chromatography quadrupole time-of-flight mass spectrometry, *J. Pharm. Biomed. Anal.*, 2013, **85**, 169–178.
- 52 A. R. Ribeiro, B. SuresT and C. Schmidt, Cephalosporin antibiotics in the aquatic environment: A critical review of occurrence, fate, ecotoxicity and removal technologies, *Environ. Pollut.*, 2018, **241**, 1153–1166.
- 53 P. F. Cuevas-Gonzalez, P. Y. Heredia-Castro, J. I. Mendez-Romero, A. Hernandez-Mendoza, R. Reyes-Diaz, B. Vallejo-CordobaA and F. Gonzalez-Cordova, Artisanal Sonoran cheese (Cocido cheese): an exploration of its production process, chemical composition and microbiological quality, *J. Sci. Food Agric.*, 2017, **97**, 4459–4466.
- 54 H. C. M. Santos, H. L. Maranduba, J. A. D. NetoL and B. Rodrigues, Life cycle assessment of cheese production process in a small-sized dairy industry in Brazil, *Environ. Sci. Pollut. Res.*, 2017, **24**, 3470–3482.
- 55 A. Tekin and Z. Guler, Glycolysis, lipolysis and proteolysis in raw sheep milk Tulum cheese during production and ripening: Effect of ripening materials, *Food Chem.*, 2019, **286**, 160–169.
- 56 R. Gaglio, M. L. Scatassa, M. Cruciata, V. Miraglia, O. Corona, R. Di Gerlando, B. Portolano, G. Moschetti and L. Settanni, In vivo application and dynamics of lactic acid bacteria for the four-season production of Vastedda-like cheese, *Int. J. Food Microbiol.*, 2014, **177**, 37–48.
- 57 D. Pangallo, N. Sakova, J. Korenova, A. Puskarova, L. Krakova, L. Valik and T. Kuchta, Microbial diversity and dynamics during the production of May bryndza cheese, *Int. J. Food Microbiol.*, 2014, **170**, 38–43.
- 58 C. Kerth, Determination of volatile aroma compounds in beef using differences in steak thickness and cook surface temperature, *Meat Sci.*, 2016, **117**, 27–35.
- 59 O. P. Soladoye, P. Shand, M. E. R. Dugan, C. Garipey, J. L. Aalhus, M. Estevez and M. Juarez, Influence of cooking methods and storage time on lipid and protein oxidation and heterocyclic aromatic amines production in bacon, *Food Res. Int.*, 2017, **99**, 660–669.
- 60 I. Bertrand, J. F. Schijven, G. Sanchez, P. Wyn-Jones, J. Ottoson, T. Morin, M. Muscillo, M. Verani, A. Nasser, A. M. D. Husman, M. Myrmel, J. Sellwood, N. Cook and C. Gantzer, The impact of temperature on the inactivation



- of enteric viruses in food and water: a review, *J. Appl. Microbiol.*, 2012, **112**, 1059–1074.
- 61 A. O. Kucukozet and M. K. Uslu, Cooking loss, tenderness, and sensory evaluation of chicken meat roasted after wrapping with edible films, *Food Sci. Technol. Int.*, 2018, **24**, 576–584.
- 62 Y. Wada and B. Lonnerdal, Effects of Different Industrial Heating Processes of Milk on Site-Specific Protein Modifications and Their Relationship to *in Vitro* and *in Vivo* Digestibility, *J. Agric. Food Chem.*, 2014, **62**, 4175–4185.
- 63 K. Heinrich, D. Chan, R. J. Fussell, J. F. Kay and M. Sharman, Can the unauthorised use of ceftiofur be detected in poultry?, *Food Addit. Contam., Part A*, 2013, **30**, 1733–1738.
- 64 L. Durel, G. Gallina and T. Pellet, Assessment of ceftiofur residues in cow milk using commercial screening test kits, *Vet. Rec. Open*, 2019, **6**, e000329.
- 65 Y. Shao, Z. Chen and L. Wu, Oxidative Stress Effects of Soluble Sulfide on Human Hepatocyte Cell Line LO2, *Int. J. Environ. Res. Public Health*, 2019, **16**, 1662.
- 66 H. Luo, L. Zhai, H. Yang, L. Xu, J. Liu, H. Liang and H. Tang, Dichloroacetonitrile induces cytotoxicity through oxidative stress-mediated and p53-dependent apoptosis pathway in LO2 cells, *Toxicol. Mech. Methods*, 2017, **27**, 575–581.
- 67 C. Cui, X. Zhang, Y. Wang, S. Y. Lu, H. J. Lu, Q. Hui, W. Ahmad, Y. Cai, X. L. Liu, L. J. Liu, F. F. Shi, Y. Y. Liu, K. Zhao, F. F. Zhai, Y. Z. Xiang, P. Hu, Y. S. Li, H. L. Ren, N. Y. Jin and Z. S. Liu, Acute and chronic toxicity assessment of benzylpenicillin G residue in heat-treated animal food products, *Chemosphere*, 2018, **202**, 757–767.

